ISSN 1063-7737, Astronomy Letters, 2023, Vol. 49, No. 12, pp. 824–832. © Pleiades Publishing, Inc., 2023.
Russian Text © The Author(s), 2023, published in Pis'ma v Astronomicheskii Zhurnal, 2023, Vol. 49, No. 12, pp. 888–896.

Neutrino Emission of Neutron-Star Superbursts

A. D. Kaminker[1*], A. Yu. Potekhin[1], and D. G. Yakovlev[1]

[1] *Ioffe Institute, St. Petersburg, Russia*

Received September 17, 2023; revised November 21, 2023; accepted November 21, 2023

Abstract—Superbursts of neutron stars are rare but powerful events explained by the explosive burning of carbon in the deep layers of the outer envelope of the star. In this paper we perform a simulation of superbursts and propose a simple method for describing the neutrino stage of their cooling, as well as a method for describing the evolution of the burst energy on a scale of several months. We note a universal relation for the temperature distribution in the burnt layer at its neutrino cooling stage, as well as the unification of bolometric light curves and neutrino heat loss rates for deep and powerful bursts. We point out the possibility of long-term retention of the burst energy in the star's envelope. The results can be useful for interpretation of superburst observations.

DOI: 10.1134/S1063773723120034

Keywords: *neutron stars, X-ray astronomy.*

1. INTRODUCTION

Neutron stars (NSs) exhibit explosive activity of various types. In particular, the bursts of accreting NSs are explained by explosive nuclear burning in their outer envelopes. Comparison of observations with theoretical models allows one to obtain useful information on the physical conditions in exploding layers, on accretion regimes, masses and radii of the NSs, the equation of state of superdense matter in NS cores, and much more (see, e.g., in 't Zand 2017; Galloway and Keek 2021).

Accreting NSs in binary systems demonstrate X-ray bursts caused by explosions of accreted hydrogen and helium under the very surface of the star, as well as much rarer but stronger superbursts (SBs) initiated by an explosion of carbon (^{12}C) in deeper layers; see, e.g., a review by in 't Zand (2017).

In this paper we consider the SBs. They have been actively modeled for more than twenty years with an account of accretion dynamics, chains of nuclear reactions, various mechanisms of heat transport, neutrino cooling, etc. (see, e.g., Cumming and Macbeth 2004; Cumming et al. 2006; Keek and Heger 2011; Altamirano et al. 2012; Keek et al. 2012, 2015).

SBs occur in deep layers of the outer envelope of an NS (e.g., Haensel et al. 2007). The envelope extends from the NS surface to the neutron-drip density of the matter ($\rho_{\rm drip} \approx 4.3 \times 10^{11}$ g/cm^3). The thickness of the envelope is several hundred meters, and its mass is $\sim 10^{-5}\ M_\odot$. It consists mainly of electrons and ions (partially or completely ionized atomic nuclei), with the ions forming a crystal, liquid, or gas.

In particular, we are interested in neutrino cooling of the SBs. Previously, it was included in calculations but was not studied systematically. In addition, we will analyse the dynamics of the evolution of the SB energy over several months and pay attention to the possibility of retaining the burst energy in the star for a long time.

2. THE PROBLEM AND NUMERICAL CODE

It is well known (e.g., Keek and Heger 2011; Altamirano et al. 2012; Keek et al. 2012, 2015) that the actual burst is preceded by the stage of formation of carbon (^{12}C) due to hydrogen-helium burning in the outermost layers of an NS. The matter containing carbon gradually accumulates and sinks into the envelope under the weight of newly accreted matter, and it reaches explosive ignition conditions at the bottom of the carbon layer with a density of $\rho_{\rm ign}$ and temperature $T_{\rm ign}$ (e.g., Keek and Heger 2011). Following the ignition, a rapid (lasting several minutes) nuclear burning occurs in a wide carbon layer, $\rho_{\rm min} \le \rho \le \rho_{\rm ign}$, where $\rho_{\rm min}$ is a density at its outer boundary. The explosion power is determined by the parameter $Q_{\rm b}$, equal to the produced energy per one nucleon; $Q_{\rm b}$ may vary depending on the conditions

*E-mail: kam@astro.ioffe.ru

of the problem. According to calculations, a carbon-containing matter burns out during an explosion into the iron group elements.

According to the theory, the maximum ignition density is limited by $\rho_{\rm ign,9} = \rho_{\rm ign}/(10^9\ {\rm g/cm^3}) \lesssim 5$, because the ^{12}C nuclei cannot survive at higher ρ due to pycnonuclear reactions and beta-captures (e.g., Shapiro and Teukolsky 1983).

After the explosion, thermal relaxation of the heated layer occurs, observable in the light curves for several hours or days. However, the internal thermal relaxation can last more than a year (e.g., Keek and Heger 2011). It is determined by the diffusion of the released heat to the surface and inside the NS, and by neutrino cooling of the heated matter.

To simulate an SB, we used a numerical code developed for studying the cooling of NSs on various spatial and temporal scales, which includes modern microphysics of the NS matter (Potekhin and Chabrier 2018). A feature of this code, which manifests itself when modeling the propagation of heat in the outer envelopes of NSs for relatively short times, is an accurate account of the removal of electron degeneracy with decreasing density or increasing temperature. The thermal evolution of the entire star is calculated, although the temperature of the core is almost unchanged during observations. We do not pretend to perform a complete self-consistent SB modeling, but make several simplifications, whose validity is discussed below.

We do not study the evolution of accreted matter in the NS envelope before the burst, such as the dynamics of ignition, formation and propagation of a shock wave, and related phenomena (e.g., Keek and Heger 2011). We assume that the burst occurs in a layer $\rho_{\rm min} \le \rho \le \rho_{\rm ign}$, where $Q_{\rm b}$ does not depend on density ρ. The quantities $\rho_{\rm min}$, $\rho_{\rm ign}$, $Q_{\rm b}$, and $T_{\rm ign}$ are treated as free parameters. The SB energy is mainly released near the ignition density $\rho_{\rm ign}$; hence the results are insensitive to $\rho_{\rm min}$, if $\rho_{\rm min} \ll \rho_{\rm ign}$ (for certainty, we fixed $\rho_{\rm min} = 10^7\ {\rm g/cm^3}$). The initial temperature profile corresponded to the thermal quasi-equilibrium in a cooling NS at $T_{\rm ign} \sim (1{-}5) \times 10^8$ K. At any density ρ in the chosen layer, the burst energy was released uniformly over time for 100 s (in the local reference frame), after which the energy release stopped. We varied $\rho_{\rm ign,9}$ from 0.1 to 5.

The values introduced above are determined in the local reference frame of the NS outer envelope. The values in the system of a remote observer will be hereafter marked by a tilde. We emphasize that everywhere (in the figures and in the text), except for Section 3, t means coordinate Schwarzschild time. In Section 3 however, the time in the local reference frame of the NS envelope is introduced; this is taken into account when comparing with the results of other sections.

3. PURE NEUTRINO COOLING

It is convenient to describe the initial post-explosion period of the cooling of the heated layer in a simple approximation of pure neutrino cooling. It is sufficient to use the well-known approximation of instantaneous explosion (e.g., Altamirano et al. 2012), assuming the temperature in the burning layer at any density ρ adiabatically reaches its maximum value $T_{\rm max}(\rho)$. Then the neutrino emission cools any matter element independently according to the equation

$$C\frac{\partial T}{\partial t} = -Q_\nu, \qquad (1)$$

where C is the heat capacity (at constant pressure P) per unit volume, and Q_ν is the neutrino energy production rate in this volume. The main neutrino processes in SBs are the neutrino emission due to Langmuir plasmon decays and the annihilation of electron-positron pairs into neutrino pairs. The solution of Eq. (1),

$$t = \int_T^{T_{\rm max}} \frac{C(T')}{Q_\nu(T')}\, dT', \qquad (2)$$

depends (parametrically) only on the values of ρ and $Q_{\rm b}$ in the given matter element; therefore, $T = T(t, \rho, Q_{\rm b})$. This solution is not sensitive to an NS model (mass, radius, equation of state) and radically simplifies the study of the neutrino stage of an SB cooling. However, when heat diffusion becomes important (see, e.g., Yakovlev et al. 2021), the noted universality is violated.

Let us add that, when modeling SBs, the column depth of matter y (g/cm^2) is often used instead of the mass density ρ, and the column depth of the burst energy $E_{\rm i}$ (erg/cm^2) is often used instead of $Q_{\rm b}$. But the solution (2) is insensitive to the NS model just when using the quantities ρ and $Q_{\rm b}$. One such solution is easily applicable to any model. In this sense, the temperature distributions at the neutrino stage of an SB are universal for different NS models.

This property is useful for testing calculations carried out with a computer code. In addition, the solution (2) can in principle be used in the code itself to speed up calculations at the neutrino stage of an SB.

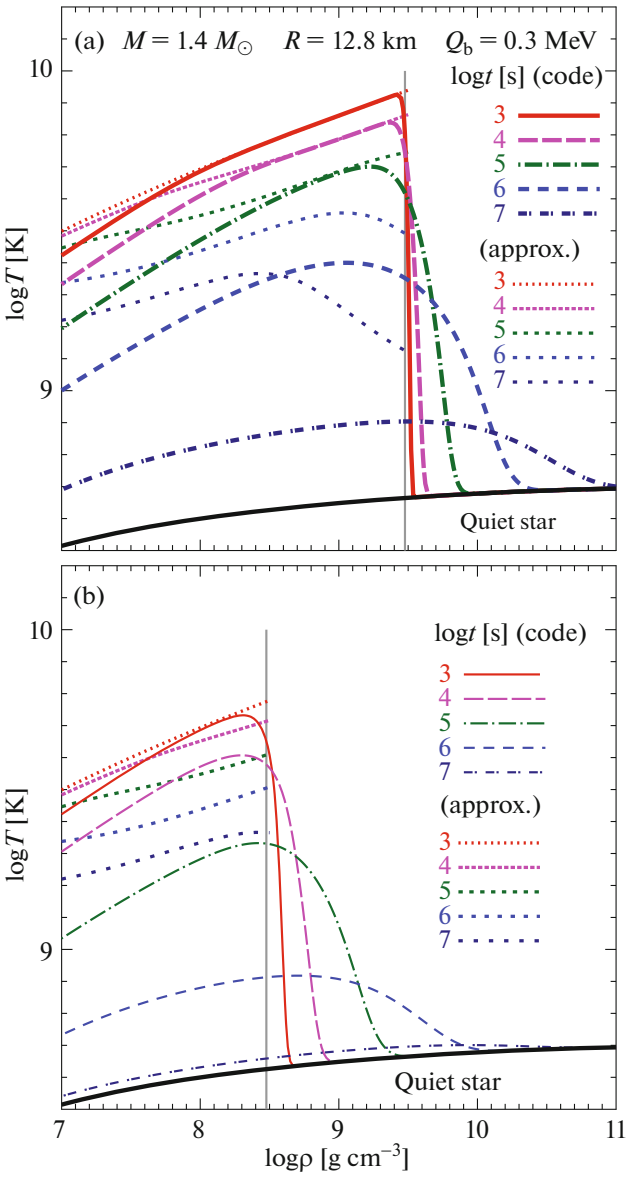

Fig. 1. The internal temperature T versus mass density ρ in the burst area at different times t for $Q_b = 0.3$ MeV and two ignition depths: (a) $\rho_{ign,9} = 3$ (thick curves) and (b) $\rho_{ign,9} = 0.3$ (thin curves). The dotted lines show the neutrino cooling approximation; they are truncated at $\rho > \rho_{ign}$ (at $\rho < \rho_{ign}$ the dotted curves in the cases (a) and (b) coincide) to the right of the vertical lines.

4. RESULTS

We present the results of SB modeling with the numerical code and compare them, where possible, with the approximation of pure neutrino cooling. In the figures below (except for Fig. 6) we have used a model of an NS with mass of 1.4 $M_\odot$. The inner crust and the core are described by the equation of state BSk24 (Pearson et al. 2018), and the outer crust consists of iron ^{56}Fe (the radius of such a star is 12.8 km); we have also considered other models and obtained similar results.

Figure 1 shows the profiles $T(\rho)$ in and near the exploded layer for two SBs at different moments of time $t \leq 10^7$ s in the reference frame of the outer envelope. Figure 1a corresponds to $\rho_{ign,9} = 3$ and Fig. 1b to $\rho_{ign,9} = 0.3$ at the same $Q_b = 0.3$ MeV. The curves are marked with the values of log t [s]. Upper curves ($t = 1000$ s, shortly after the SB) are close to the thermodynamic curve $T_{max}(\rho)$, which is the same at a fixed Q_b. Note the sharp breaks in $T_{max}(\rho)$ at $\rho \approx \rho_{ign}$. The spreading of heat from the explosion area gradually turns the break into a blurred maximum, with the heat diffusing into the NS at larger depths and outwards at lower ρ.

The dotted lines in Figs. 1a and 1b show the temperature profiles for pure neutrino cooling. In case (a) of deep ignition ($\rho_{ign,9} = 3$), this approximation works well in the layer where the main burst energy has been produced ($\rho_9 \gtrsim 0.3$) during $t \lesssim (1–3) \times 10^5$ s. With the pure neutrino cooling, the temperature profiles $T(\rho, t)$ are universal and can be easily obtained without using the cooling code. In case (b) of a shallower ignition ($\rho_{ign,9} = 0.3$), the neutrino cooling stage turns out to be much shorter ($t \lesssim 10^3$ s) and practically insignificant (see below). Thus, the approximate solutions coincide with the exact ones in the cases in which the cooling of matter is determined by neutrino radiation, i.e., at sufficiently short times of deep and powerful bursts.

When the temperature $T(\rho)$ drops, the neutrino cooling approximation is violated. So, in a layer with an arbitrary density ρ, the neutrino cooling becomes insignificant at sufficiently low Q_b, at which $T(\rho) \lesssim T_\nu$. Here $T_\nu \sim (3–4) \times 10^9$ K is a characteristic temperature that is weakly dependent on ρ. This circumstance has been repeatedly noted in the literature (e.g., Cumming and Macbeth 2004; Cumming et al. 2006).

As an example, in Fig. 2 we show the evolution of temperature $T(t)$ in four SBs with different heat releases ($Q_b = 0.05–0.3$) and with ignition either at $\rho_{ign,9} = 3$ (thick lines), or at $\rho_{ign,9} = 0.3$ (thin lines). At each value of ρ_{ign} the profiles $T(t)$ are shown for the layer with density $\rho = 0.8\,\rho_{ign}$.

It is remarkable that the cooling curves $T(t)$ for the two most powerful SBs ($\rho_{ign,9} = 3$, $Q_b \gtrsim 0.2$) at $t \gtrsim 10^4–10^5$ s merge into the same "universal" curve. This effect is well known in the theory of neutrino cooling of NSs (e.g., Yakovlev and Pethick 2004) as the "memory loss" of initial conditions because of a strong dependence of the neutrino cooling rate

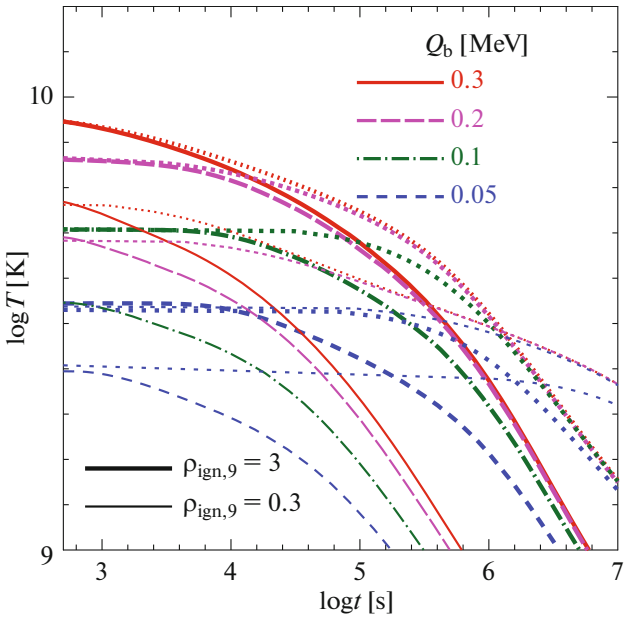

Fig. 2. The dependence $T(t)$ for the two ignition models in Fig. 1 in the layers with $\rho = 0.8\rho_{ign}$ at $Q_b = 0.3$, 0.2, 0.1, and 0.05 MeV. Solid, dashed, and dot-dashed lines correspond to the numerical simulations; dotted lines show the neutrino cooling approximation. Here and hereafter, the end of heating in the layer (ρ_{min}, ρ_{ign}) is taken as the starting point $t = 0$.

on temperature: a noticeable excess of T over T_ν causes rapid neutrino cooling down to $T \sim T_\nu$, which "unifies" the cooling. If we increase Q_b to still higher values, then the additional burst energy will be carried away by neutrinos, and the dependence $T(t)$ at $t \gtrsim 10^5$ s will not change.

However, in other cases, considered in Fig. 2, the neutrino cooling (at $\log t \gtrsim 4$) turns out to be so weak that it does not actually affect $T(t)$.

Figures 3a and 3b present bolometric neutrino and electromagnetic light curves, $\widetilde{L}_\nu(t)$ and $\widetilde{L}_\gamma(t)$, for the same SB models as in Fig. 2. A comparison of $\widetilde{L}_\nu(t)$ and $\widetilde{L}_\gamma(t)$ shows that for the shallower depth ($\rho_{ign,9} = 0.3$) the photon luminosity $\widetilde{L}_\gamma(t)$ dominates at all the chosen values of Q_b (except for the earliest moments after the nuclear burning). In the deeper burst ($\rho_{ign,9} = 3$), especially with high Q_b (0.3 and 0.2 MeV), on the contrary, the neutrino heat outflow becomes decisive. Merging of the curves $\widetilde{L}_\nu(t)$ at $Q_b = 0.3$ and 0.2 confirms the conclusion on the unification of cooling of deep and powerful SBs at $t \gtrsim 3 \times 10^4$ s as a result of powerful neutrino emission.

Dotted lines in Fig. 3a show the dependences $\widetilde{L}_\nu(t)$, calculated in the approximation of pure neutrino cooling. They are obtained by integrating neutrino emissivities $Q_\nu(\rho, t)$ over the volume of the exploded layer in the NS envelope. A comparison with the results of accurate calculations confirms the conclusions on the duration and efficiency of the neutrino cooling stage drawn from the analysis of Figs. 1 and 2.

The electromagnetic light curves shown in Fig. 3b are formed after the heat wave from the burning layer has reached the surface (e.g., Cumming and Macbeth 2004; Keek and Heger 2011; Keek et al. 2012). The initial segments of these curves are determined by the outer parts of this layer ($\rho \sim \rho_{min}$), while later parts of the light curves are determined by deeper layers where most of the energy is released ($\rho \sim \rho_{ign}$). However, at the early stage, the dependences $T(\rho)$ at the same Q_b are rather close to each other (Fig. 1). Therefore, the early segments ($t \sim 10^2$–10^4 s) of the light curves $\widetilde{L}_\gamma(t)$ for the SBs with such Q_b weakly differ from each other (Fig. 3b). The bursts with $\rho_{ign,9} = 0.3$ are shorter than the deeper bursts with $\rho_{ign,9} = 3$. The similarity of the curves $\widetilde{L}_\nu(t)$, as well as of the curves $\widetilde{L}_\gamma(t)$, for the deeper SBs at $Q_b = 0.3$ and 0.2 MeV at late stages ($t \gtrsim 10^4$ s) is explained by the same unifying influence of powerful neutrino heat outflow at the beginning of SBs.

Figure 4 presents the light curves $\widetilde{L}_\gamma(t)$, computed for the bursts with $Q_b = 0.3$ MeV at six ignition depths $\rho_{ign,9}$ from 0.1 to 5. At $t \lesssim 1000$ s, all the curves almost coincide; later they differ but have common properties. We can see that with the growth of ρ_{ign}, the duration of the afterglow of the SB increases, which is associated with prolonging heat diffusion from deeper layers to the NS surface (e.g., Yakovlev et al. 2021).

Note that our calculations allow us to study the evolution of the thermal energy of an SB. The total energy of the SB, E_{tot}, is released already a few minutes after the SB start in a layer of burnt carbon. Having known from the simulations, the photon $L_\gamma(t)$ and neutrino $L_\nu(t)$ luminosities of the NS, as well as luminosities $L_{\gamma 0}$ and $L_{\nu 0}$ in the quiescent NS (before the SB), we find the luminosities $L^*_\gamma = L_\gamma - L_{\gamma 0}$ and $L^*_\nu = L_\nu - L_{\nu 0}$, which are determined by the SB itself. Integrating them over time from the start of the heating to the current moment t, we obtain the photon and neutrino energies of the SB, $E^*_\gamma(t)$ and $E^*_\nu(t)$, that have been taken away from the star by any current time moment t. The quantity $E^*_T(t) = E_{tot} - E^*_\gamma(t) - E^*_\nu(t)$ can be called residual thermal energy of the SB in the NS. Here, the energies and luminosities are given in the local reference frame, since all the

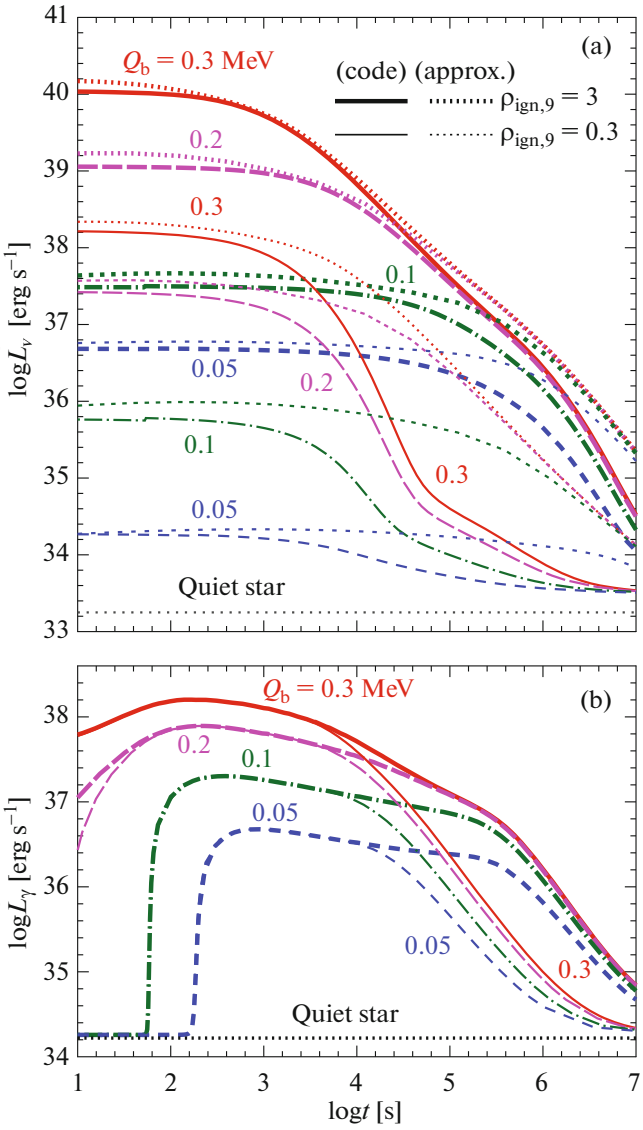

Fig. 3. Neutrino $\widetilde{L}_\nu(t)$ (a) and electromagnetic $\widetilde{L}_\gamma(t)$ (b) light curves, calculated for the same SB models as in Fig. 2. The luminosities are redshifted (for a distant observer).

main processes of thermal evolution occur in the outer crust, which is so thin that space-time is almost flat in it, although with different time and spatial scales than in the system of a remote observer.

Figure 5 gives examples of time-dependences $E^*_\gamma(t)$, $E^*_\nu(t)$, and $E^*_{tot}(t)$ for six SBs at three values of $\rho_{ign,9} = 0.3$ (Fig. 5a), 1 (Fig. 5b), and 3 (Fig. 5c). Two bursts are considered for each ignition density, with sufficiently low ($Q_b = 0.1$ MeV) and high ($Q_b = 0.3$ MeV) fuel efficiencies. The solid horizontal lines show full energies of the SBs. The active phase of the SB energy removal continues longer for higher ρ_{ign}.

Figure 5a shows the dependences for shallower bursts. We see that, at a weak SB ($Q_b = 0.1$ MeV), the neutrino cooling is negligible. The main relaxation mechanism of such SB is the emission of photons from the surface. However, even after 10^7 s, when the afterglow from the surface is hardly observable, there remains over 10^{41} ergs of the SB energy in the NS. A more powerful burst ($Q_b = 0.3$ MeV) at this depth is accompanied by considerably stronger neutrino cooling, which, nevertheless, is comparable in intensity with the photon cooling during ~1000 s, and weakens afterwards. Meanwhile the photon cooling remains powerful, and in 10^7 s it scoops out a significant fraction of E_{tot}.

Figure 5b corresponds to two SBs at a moderate depth $\rho_{ign,9} = 1$. The neutrino cooling of the weaker burst ($Q_b = 0.1$ MeV) is inefficient, so that the most

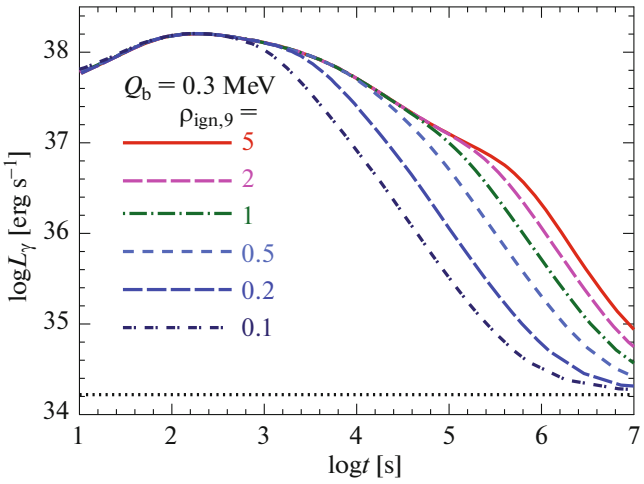

Fig. 4. Photon light curves $\widetilde{L}_\gamma(t)$ for superbursts, calculated for $Q_b = 0.3$ MeV, at different ignition depths $\rho_{ign,9}$, from 0.1 to 5.

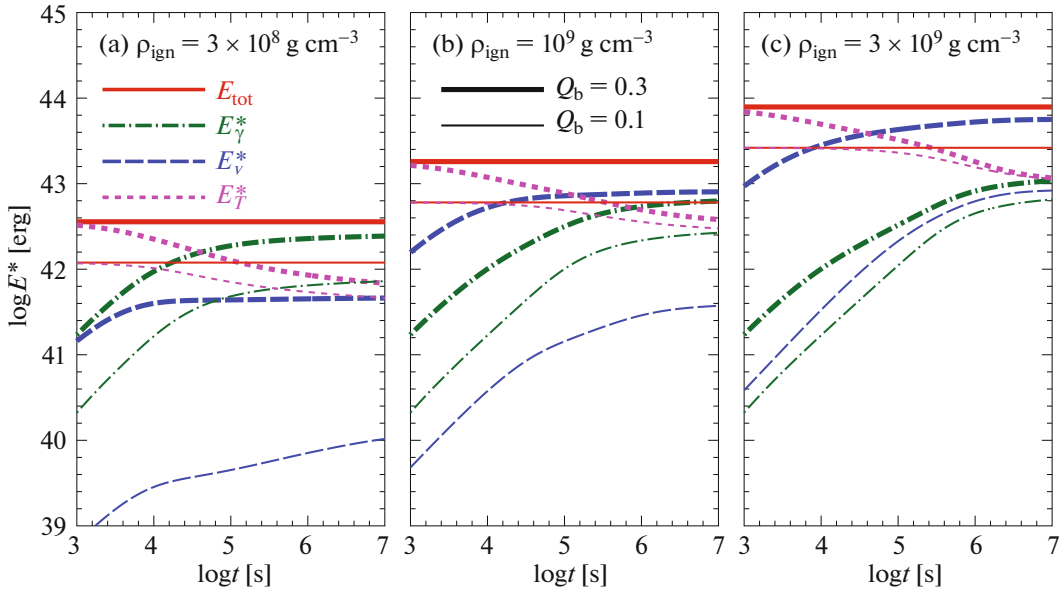

Fig. 5. The evolution of the thermal energy of SBs in time, calculated at $\rho_{ign,9} = 0.3$ (a), 1 (b), and 3 (c) in the cases of $Q_b = 0.3$ MeV (thick lines) and 0.1 MeV (thin lines): E^*_γ is the energy of the SB that is radiated through the star's surface, E^*_ν is the radiated neutrino energy of the SB, E^*_T is the residual energy of the SB in the NS. The solid horizontal lines show the full energy of the burst E_{tot}.

of the energy is carried out by radiation through the surface. By the moment $t = 10^7$ s, there still remains $\sim 10^{42}$ ergs of the SB energy in the NS. At a stronger burst ($Q_b = 0.3$ MeV), on the contrary, the excess energy is carried away mainly by neutrinos, but the residual energy remains very large.

Figure 5c demonstrates two SBs with the ignition depth of ^{12}C, which is close to the limiting one. The weaker SB differs from the weaker SBs in Figs. 5a and 5b: now the neutrino heat loss dominates over the heat loss through the surface, although the difference between the heat losses through these two channels is small. Meanwhile, the residual energy by the moment $t = 10^7$ s is only a few times smaller than the total energy E_{tot}. Our estimates show that in this case the main part of this energy flows into the star.

Finally, the stronger burst ($Q_b = 0.3$ MeV) in Fig. 5 is accompanied by an unusually powerful neutrino heat outflow. This burst belongs to a special class of carbon superbursts, which are almost entirely controlled by neutrino processes. According to the calculations, the rate of heat transport inside the

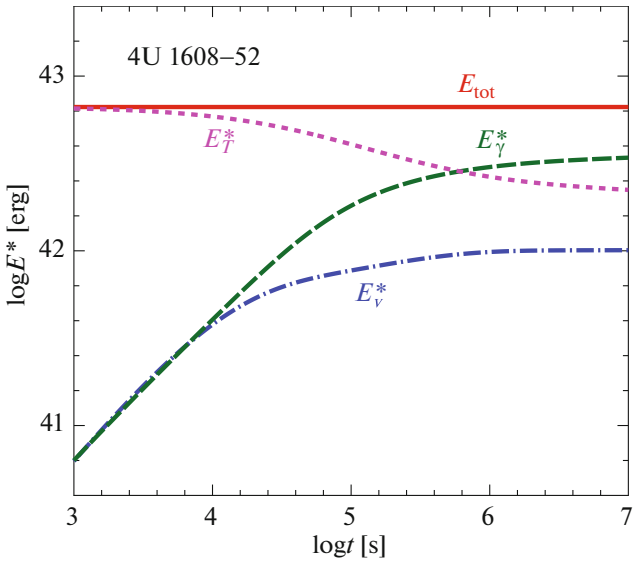

Fig. 6. The evolution of thermal energy of the powerful NS burst in the X-ray source 4U 1608–52, calculated for SB parameters taken from interpretation of its observations.

star significantly exceeds the rate of energy outflow through the surface. The possibility of implementing such bursts in the NSs is not yet clear.

As an example, in Fig. 6 we have depicted the thermal evolution of the SB of the transiently accreting NS in the low-mass X-ray binary system 4U 1608–52. The burst was observed on May 5, 2005, by the instrument "All-Sky Monitor" onboard the *Rossi X-ray Timing Explorer* space observatory. The analysis of the observations (e.g., Keek et al. 2008; in 't Zand 2017) shows that it was apparently one of the most powerful and deepest superbursts. For an NS with $M = 1.4\ M_\odot$ and $R = 10$ km, fitting of the observed X-ray light curve by theoretical models gave (in our notation) $\rho_{\rm ign,9} \approx 1.3$, $Q_{\rm b} \approx 0.17$ MeV.

Figure 6 presents results of our calculations for this burst (with the indicated NS parameters) in the same form as in Fig. 5. The neutrino radiation effectively cools the SB for a relatively short time. For several hours, the neutrino cooling rate is (coincidentally) close to the rate of photon emission through the NS surface. Later, the photon cooling from the NS surface dominates, but by $t = 10^7$ s (about 4 months) it becomes weak too. During this time, the neutrinos carry away about a quarter of the total energy of the burst and the photons radiate away about 60% of it. The residual thermal energy is $\gtrsim 10^{42}$ erg.

These results, as well as the results presented in Fig. 5, indicate that even a few months after an SB, a significant part of the explosion energy may remain in the star. Calculations show that this energy (especially for deep SBs) largely flows into the deep layers of a NS. The question of the further history of this energy is not trivial. For example, in the presence of regularly recurring bursts, their heat gradually warms up the entire star. It is possible to choose the frequency or intensity of the bursts so that, in general, the star remains in a quasi-stationary state (e.g., Colpi et al. 2001; Keek and Heger 2011). The evolution of residual heat can be determined by small and rather complex temperature gradients in the NS envelope, which can appear there for various reasons. This issue requires further study.

In addition, we have performed a series of simulations of NS superbursts with different equations of state of superdense matter, with varying the mass (and radius) of the star, as well as other parameters of the problem, including $\rho_{\rm min}$ and $T_{\rm ign}$. The use of different equations of state and NS parameters did not reveal qualitatively new effects. Reducing $\rho_{\rm min}$ below the adopted value 10^7 g/cm^3 (which is quite acceptable; see, e.g., Keek and Heger 2011; Keek et al. 2012; Altamirano et al. 2012) cannot noticeably change the global SB evolution. It can affect very early segments of photon light curves, which we do not model anyway. Variations of the ignition temperature $T_{\rm ign}$ also have a weak effect on the SB model as long as this temperature is noticeably lower than the temperature of the heated matter after the explosion. The ignition temperature can be determined self-consistently for each individual burst. However, a self-consistent calculation is complicated and requires not always reliably known microphysics (for example, the rates of many reactions that accompany the carbon burning). The conclusion that the results of our simplified modeling are not sensitive to the exact values of $T_{\rm ign}$ confirms the adequacy of our approach.

Whenever possible, we tried to compare our results with the results of other authors. In particular, we obtained a good agreement with Fig. 2 in the paper by Cumming et al. (2006), where the neutrino and photon cooling rates after a burst were compared, and with Fig. 5 in the paper by Keek and Heger (2011), where the dependences $L_\gamma(t)$ and $L_\nu(t)$ were presented for one of SBs.

5. CONCLUSIONS

We have considered the main features of rare and very energetic events, the superbursts, occurring in deep layers of the outer envelopes of accreting NSs; they are caused by the explosive combustion of accumulated carbon (^{12}C) in these layers. For their modeling, we used a numerical code (Potekhin and

Chabrier 2018) based on modern NS microphysics (Section 2), introduced the approximation of pure neutrino cooling (Section 3), and analyzed the dynamics of heat propagation during the post-burst relaxation (Section 4).

A simple method for studying the neutrino cooling stage of the outer crust is proposed, which allowed us to formulate a universal relation for the temperature distribution $T(t, \rho, Q_{\rm b})$ in the exploded layer.

It is noted that the dynamics of the SBs is determined by two main parameters: the density $\rho_{\rm ign}$ of explosive ignition of carbon and the fuel energy $Q_{\rm b}$ deposited per nucleon. At rather shallow SBs ($\rho_{\rm ign,9} \lesssim 0.3$) the neutrino cooling turns out to be insignificant for any considered $Q_{\rm b}$; one can call such SBs "neutrinoless." With increasing $\rho_{\rm ign}$ at sufficiently high $Q_{\rm b}$, the neutrino cooling is beginning to be important. The duration of neutrino cooling stage is increasing (from $\sim 10^3$ s at $\rho_{\rm ign,9} \sim 0.3$ to $\gtrsim 10^5$ s at $\rho_{\rm ign,9} \sim 3$). With growing $Q_{\rm b}$ to $\sim$0.3 MeV, the SB-generated neutrino luminosity $L_\nu(t)$ starts to exceed the photon luminosity $L_\gamma(t)$ from the NS surface, taking control of the cooling. At especially deep ignitions $\rho_{\rm ign,9} \gtrsim 3$ and high $Q_{\rm b} \sim 0.3$ MeV, the main fraction of the SB energy is carried away by neutrinos, and the light curve $L_\gamma(t)$ is determined by only a small fraction of the SB energy. Moreover, with increasing $\rho_{\rm ign}$, more and more energy is carried by thermal conduction inside the NS. In certain cases, a fairly large burst energy can remain in the star even a few months after the SB.

The employed cooling code facilitates simulations of the evolution of burst energy over time (Fig. 5). A comparison with observations can help one to study the dynamics of SB energy for specific events (Fig. 6).

Once again, we emphasize that SB modeling has been performed at an advanced level for more than 20 years (see, e.g., Cumming and Macbeth 2004; Cumming et al. 2006; Keek and Heger 2011; Altamirano et al. 2012; Keek et al. 2012, 2015; in 't Zand 2017; Galloway and Keek 2021, and references therein). Many of the results mentioned above (for example, the possibility of removing a large fraction the SB energy by neutrinos) were obtained earlier (see, e.g., Cumming et al. 2006; Keek and Heger 2011). Our consideration allowed us to determine a number of general features of the SBs. These include: a simplified description of the neutrino cooling stage of the outer crust; the possibility of studying the evolution of SB thermal energy on scales of several months and the conclusion on possibility of retaining SB energy inside the star on such time scales.

The maximal ignition depths $\rho_{\rm ign,9} \sim 5$ considered here are perhaps limiting for the explosive burning of ^{12}C (see, e.g., Potekhin and Chabrier 2012). However, one cannot exclude that bursts due to burning of matter with different composition are possible in still deeper layers. For instance, Page et al. (2022) suggested that the powerful bursting activity of the X-ray source MAXI J0556−332 is related to a hyperburst in an NS at $\rho_{\rm ign,9} \sim 100$ (near the boundary of the outer envelope and inner crust) as the effect of explosive burning of a number of isotopes with large neutron excesses. According to the theory, such hyperbursts, if they occur, are very rare. If they do occur, they represent a continuation of the family of ordinary carbon superbursts, but in an extremely unusual mode.

Our results can also be useful for studies of conventional thermonuclear bursts in the surface layers of NSs. First of all, these are the so-called intermediate duration bursts, which are shorter than the SBs. They occur in a helium layer on cold NSs (see, e.g., Cumming et al. 2006; in 't Zand 2017). Similar energy transfer problems occur with SBs or ordinary bursts of magnetars in their inner or outer crusts under the influence of superstrong magnetic fields (e.g., Kaspi and Beloborodov 2017).

FUNDING

The work was supported by the Russian Science Foundation (grant no. 19-12-00133-P).

CONFLICT OF INTEREST

The authors of this work declare that they have no conflicts of interest.

REFERENCES

1. D. Altamirano et al., Mon. Not. R. Astron. Soc. **426**, 927 (2012).
2. M. Colpi, U. Geppert, D. Page, and A. Possenti, Astrophys. J. **548**, L178 (2001).
3. A. Cumming and J. Macbeth, Astrophys. J. **603**, L37 (2004).
4. A. Cumming, J. Macbeth, J. J. M. in 't Zand, and D. Page, Astrophys. J. **646**, 429 (2006).
5. G. K. Galloway and L. Keek, *Timing Neutron Stars: Pulsations, Oscillations, and Explosions,* Ed. by T. M. Belloni, M. Mendez, and C. Zang, Vol. 461 of *Astrophysics Space Sci. Library* (Springer, Berlin, 2021), p. 209.
6. P. Haensel, A. Y. Potekhin, and D. G. Yakovlev, *Neutron Stars. 1. Equation of State and Structure* (Springer, New York, 2007).
7. V. M. Kaspi and A. M. Beloborodov, Ann. Rev. Astron. Astrophys. **55**, 261 (2017).
8. L. Keek and A. Heger, Astrophys. J. **743**, 189 (2011).
9. L. Keek, J. J. M. in 't Zand, E. Kuulkers, A. Cumming, E. F. Brown, and M. Suzuki, Astron. Astrophys. **479**, 177 (2008).

10. L. Keek, A. Heger, and J. J. M. in 't Zand, Astrophys. J. **752**, 150 (2012).
11. L. Keek, A. Cumming, Z. Wolf, D. R. Ballantyne, V. F. Suleimanov, E. Kuulkers, and T. E. Strohmayer, Mon. Not. R. Astron. Soc. **454**, 3559 (2015).
12. D. Page, J. Homan, M. Nava-Callejas, Y. Cavecchi, M. V. Beznogov, N. Degenaar, R. Wijnands, and A. S. Parikh, Astrophys. J. **933**, 216 (2022).
13. J. M. Pearson, N. Chamel, A. Y. Potekhin, A. F. Fantina, C. Ducoin, A. K. Dutta, and S. Goriely, Mon. Not. R. Astron. Soc. **481**, 2994 (2018).
14. A. Y. Potekhin and G. Chabrier, Astron. Astrophys. **538**, A115 (2012).
15. A. Y. Potekhin and G. Chabrier, Astron. Astrophys. **609**, A74 (2018).
16. S. Shapiro and S. Teukolsky, *Black Holes, White Dwarfs, and Neutron Stars: The Physics of Compact Objects* (Wiley, New York, 1983).
17. D. G. Yakovlev and C. J. Pethick, Astron. Astrophys. **42**, 169 (2004).
18. D. G. Yakovlev, A. D. Kaminker, A. Y. Potekhin, and P. Haensel, Mon. Not. R. Astron. Soc. **500**, 4491 (2021).
19. J. J. M. in 't Zand, in *7 Years of MAXI: Monitoring X-ray Transients,* Ed. by M. Serino, M. Shidatsu, W. Iwakiri, and T. Mihara (RIKEN, Saitama, 2017), p. 121.